Parallel Sensing/Probing Architecture and Adaptive Protocol Design for Opportunistic Networks

Mohammad J. Abdel-Rahman, Harish Kumar Shankar, and Marwan Krunz

Technical Report
TR-UA-ECE-2015-1

***Abstract*—The proliferation of bandwidth-hungry multimedia traffic over IEEE 802.11-based WLANs has overcrowded the ISM bands. The opening of the UHF TV band by the FCC for unlicensed opportunistic operation promises to relieve the demand on ISM bands. However, supporting bandwidth-intensive applications over TV white spaces can be quite challenging, due to the unpredictable nature of spectrum availability combined with the fluctuations of channel quality. The realization of this herculean feat through unlicensed usage, whilst providing protection to licensed primary users, requires intelligent and adaptive protocol design. In this paper, we propose a QoS-aware parallel sensing/probing architecture, called QASPA, which exploits inherent channel and user diversities exhibited by the wireless system. Aiming at maximizing the sensing efficiency while achieving a high detection accuracy, QASPA incorporates an optimal adaptive double-threshold-based sensing mechanism. It also embodies a cross-layer protocol, which uses an adaptive framing structure to minimize the control overhead, and a novel spectrum assignment strategy targeted at improving the spatial reuse of the network. The proposed spectrum assignment strategy supports both channel bonding and aggregation. Our simulations validate the ability of QASPA in guaranteeing the demands of high-bandwidth opportunistic flows while supporting low-bandwidth flows. They also show the superior performance of QASPA compared to the scheme used in the ECMA-392 standard for opportunistic indoor streaming.**

Keywords*—*Channel allocation, channel probing, integer programming, multimedia communication, opportunistic access radio, optimal stopping theory, spectrum sensing.

I. Introduction

WIRELESS communications have witnessed tremendous growth over the last decade, placing significant demand for RF spectrum. Spectrum scarcity is only expected to worsen in time, as new wireless services make their way to the commercial world. The FCC has accordingly declared a "spectrum crisis." In the words of its Chairman Julius Genachowski, "the biggest threat to the future of mobile communications ... is the looming spectrum crisis" [1].

Traditionally, much of the spectrum is statically licensed for a given use in a given geographic area. Exceptions to this norm include the ISM bands, which facilitate many indoor and short-range communications (e.g., WLANs, Bluetooth, etc.). However, these bands are reaching their capacity limit, as more bandwidth-hungry multimedia traffic is being pushed through them (e.g., media steaming, interactive gaming, real-time voice/video calling, etc.). Dynamic spectrum access (DSA) tries to address the spectrum crisis by allowing spectrum-agile devices with cognitive radio (CR) capabilities to operate *opportunistically* as secondary users (SUs) over certain licensed bands, including the TV white spaces (TVWS). However, supporting the quality of service (QoS) requirements of high-bandwidth applications using the DSA paradigm is a herculean feat, to say the least. These applications require sustained throughput (in bps) to maintain acceptable video quality. This can be quite difficult to guarantee in a DSA environment that is characterized by spatiotemporal variations in spectrum availability. In fact, the mere presence of spectrum holes that, on average, exhibit low primary user (PU) activity is not enough to enable bandwidth-intensive communications. One also needs to take into account the *quality* of these holes. To minimize the disruption to the high-bandwidth flows, the spectrum sensing process needs to identify *stable* idle channels, i.e., ones that are expected to remain idle for an extended period of time.

The main objective of this paper is to provide a framework for opportunistically transporting heterogeneous traffic, which includes high-bandwidth flows as well as best-effort flows, over TVWS without interfering with the operation of PUs. To this end, we design a QoS-aware parallel sensing/probing architecture called QASPA and a cross-layer protocol that encompasses all the needed components. QASPA involves five key novelties. First, it uses estimated PU activity profiles to construct a schedule for parallel (concurrent) sensing/probing of different channels, and for determining the best channel to use for control and management over the next frame. In contrast to [2], in which channel quality is inferred by periodically probing random spectral bands without any scheduling, in our scheme links are scheduled for sensing/probing such that the rate demands of prospective traffic flows are probabilistically guaranteed to be satisfied.

Second, QASPA adopts an adaptive TDMA-based frame structure whose objective is to minimize the control overhead and hence maximize the data-transmission period. This scheme is intended to address the deficiencies in fixed-frame protocols, including OP-MAC [3] and the one used in the ECMA-392 standard for opportunistic media streaming [4]. ECMA-392 follows a master-slave approach for managing portable/personal devices operating over TVWS. It uses a hybrid of ad hoc and infrastructure-based network architectures (see Fig. 1). Specifically, a master device acts as a centralized entity, and is responsible for coordinating associated slave

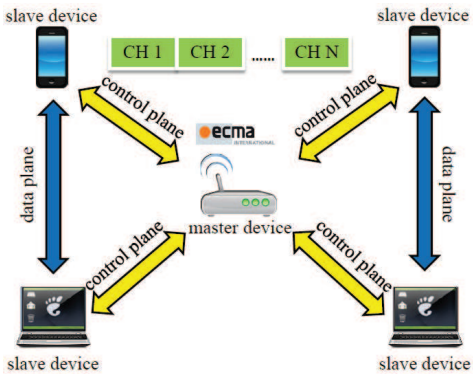

Fig. 1: Network topology used in our design.

devices by exchanging control messages with them. However, on the data plane, communications among the slave devices can take place directly or via the master device.

Third, QASPA uses a novel multi-channel sensing/probing scheme that exploits the inherent multi-user diversity of a wireless system to maximize the number of discovered opportunities over a given time period. Several schemes have been developed in the literature to maximize the spectrum utilization while limiting interference onto PUs (see, for example, [5]). These schemes do not exploit multi-user diversity, whereby the quality of a particular channel varies from one link to another. Many protocols have been proposed to improve the spatial reuse of a network (e.g., [6]–[8]). However, our problem is further complicated by the need to maximize the network's spatial reuse while guaranteeing the rate demands of high priority (HP) flows and ensuring interference-free PU communications.

Fourth, we integrate into QASPA an optimal adaptive double-threshold-based spectrum sensing algorithm, which aims at maximizing the spectrum sensing efficiency while achieving a high PU detection accuracy. In contrast to the conventional single-threshold sensing approach, double-threshold sensing schemes can simultaneously achieve low miss-detection and low false-alarm probabilities within a short sensing time [9]. However, double-threshold sensing involves an "uncertainty region:" If the sensing outcome falls between the two sensing thresholds (i.e., in the uncertainty region), the channel is considered neither busy nor idle [9]. In our work, we address this problem by adaptively adjusting the channel sensing time, so that the uncertainty region is reduced while, at the same time, the required miss-detection and false-alarm probabilities are met. In contrast to [10], in our protocol the total sensing time per frame is fixed, and the objective of our adaptive scheme is to maximize the number of discovered opportunities within the allocated sensing time, while maintaining a required detection accuracy. We formulate the optimal adaptive double-threshold-based sensing problem using optimal stopping theory [11]. Optimal stopping theory has been previously used in single-threshold-based systems to optimize the *number of sensed channels* [12]. In this paper, we use this theory to optimize the *channel sensing time*, assuming a double-threshold-based system. Unlike the cooperative sensing scheme in [13], our scheme is efficient even with a small number of operational SUs in the network. As a result, we do not compromise the sensing accuracy even when the number of operational SUs is small.

Finally, using the outcome of the channel sensing/probing process, we design a centralized spectrum assignment scheme for QASPA that supports channel bonding and aggregation, and that aims at maximizing the number of concurrently active flows. Rather than focusing on the performance of an individual link, we are interested in optimizing the overall efficiency of the entire opportunistic network.

The rest of the paper is organized as follows. In Section II, we define our network model. We provide an overview of QASPA in Section III. The adaptive frame structure is introduced in Section IV, followed by the proposed parallel sensing/probing design in Section V. In Section VI, we present the channel allocation scheme. We evaluate the proposed design in Section VII. Main conclusions are provided in Section VIII.

II. Network Model and Protocol Assumptions

We consider an opportunistic CR network (CRN) with a centralized controller, called the *master device* (MD) (see Fig. 1), which plays an analogous role to a wireless access point (AP). In contrast to a WiFi-based AP, data communications (i.e., user payload) in our setup can occur directly between any two nodes (two *slave devices*, or a slave device and the MD), whereas control information (e.g., scheduling information, channel quality reporting, etc.) can be exchanged only between a slave device and the MD. The conventional viewpoint of SU-PU coexistence is preserved, wherein SUs strive to communicate over channels that are not used by PUs. An arbitrary number of peer-to-peer (P2P) links, comprised of CR-enabled Tx-Rx pairs, become associated with the MD through appropriate signaling that occurs before initiating any data communication. Each device is equipped with a half-duplex transceiver, operating at a constant transmission power. Hence, a node can only listen to or transmit over one channel at a time. This setup is the same as the one used in the ECMA-392 architecture [4].

We classify the traffic over active P2P links into two classes: bandwidth-intensive HP flows and best-effort low priority (LP) flows. Specifically, flows with a rate demand greater than R_{th} Mbps are classified as HP, and all other flows are deemed as LP flows. The type of flow (HP/LP) carried by a link is indicated using a single bit in the association packet sent to the MD. Let $\mathcal{L}$ represent the set of HP flows in the network ($|\mathcal{L}| = L$). HP flows are assumed to be long-lived, with a stringent rate demand of $R_d^{(j)}$ for flow $j \in \mathcal{L}$. We envision separate communication paths for control and data. All control packets needed to initiate data communications along a given link are exchanged between the MD and data sender of that link. On the other hand, once the MD allocates channels for links, data exchanges take place between the respective peer devices without any intervention from the MD. All peer devices are assumed to be within the communication range of the MD, which is typically the case in indoor environments.

Let $\mathcal{N}$ ($|\mathcal{N}| = N$) denote the set of orthogonal channels in the UHF band that can be used opportunistically. We require that no two links can transmit over the same channel at the same time. The channel quality, obtained through probing, is assumed to be stationary during the channel's coherence time, denoted by $\tau_c^{(i)}$ for channel $i \in \mathcal{N}$. The channel quality is also assumed to be link-dependent. PU activity over channel i is modeled as a continuous-time Markov process, which alternates between busy and idle states, with average busy and idle durations of $T_{\text{on}}^{(i)}$ and $T_{\text{off}}^{(i)}$, respectively (see, for example, [14], [15]).

III. Protocol Overview

To support opportunistic high-bandwidth applications, we design a QoS-aware parallel sensing/probing architecture (QASPA) that uses a predefined frame length T_{frame}. Synchronization among various SUs is achieved by disseminating control packets over *a dynamically assigned* control channel (CC), which is determined on-the-fly by the MD based on the estimated PU channel-usage profile. Similar to ECMA-392, in our setup each frame consists of a number of medium access slots (MAS), reserved for various operations, including network-wide synchronization, parallel sensing/probing, concurrent data communication, etc.

QASPA follows an *adaptive* frame structure (AFS) design, whereby fields used to support various protocol operations may vary from one frame to another, even though the overall frame length is still fixed at T_{frame}. This design is intended to eliminate redundant operations, resulting in drastic reduction in the protocol overhead and improvement in the network goodput. A summary of the main functions of the proposed protocol is provided below.

Association. In line with [16], we assume the existence of an intelligent AP discovery mechanism for associating prospective P2P links with the MD and establishing a synchronized network. Once associated, links carrying HP flows provide their rate demands to the MD. Rate demands play a key role in the operation of other elements of the protocol.

Beacon Period (BP). Beacons are transmitted by the MD in two instances. First, at the beginning of each frame, the type of the TDMA frame to be used (as determined by the AFS algorithm) is broadcasted to all links in the network. Second, towards the end of the frame, the newly designated CC for the following frame period is broadcasted to the entire network. Allowing the CC to be adjusted on a per-frame basis gives great flexibility and robustness against fast PU dynamics.

Sensing/Probing Scheduling. The scheduling of concurrent sensing/probing processes forms the crux of the QASPA design. The MD schedules the channels that various links need to sense/probe during the spectrum discovery phase. Such scheduling takes into account the rate demands of HP flows and the estimated PU profiles, and attempts to maximize the number of discovered spectrum opportunities (hence, the number of active links in the network). Unlike the schemes in [2], our sensing/probing scheduling takes into account the link-dependent channel quality obtained from previous probing instances. In [2], the quality of one channel over a given link is used to infer the quality of the other channels, based on simple path-loss models. This is not accurate for indoor settings, where the effect of the prevailing multi-path conditions over the other channels.

Reporting. After sensing/probing a specified set of channels, each link reports the PU state of these channels along with their measured qualities (if detected idle) to the MD. This information is used by the MD for channel allocation.

Channel Assignment. The MD strives to maximize the number of admitted flows with satisfied rate demands (HP and LP), by incorporating channel bonding and aggregation techniques. We introduce a second round of probing to further increase the admission probability. The major motivation behind this design is to support multiple flows simultaneously, so as to increase the spatial reuse of the network.

Data Transmission. After channel assignment, links communicate in a P2P fashion over the assigned channels for a duration T_{data}, which depends on the frame type.

It is to be instilled that the BPs at the start and end of a frame are the only two recurring fields in a frame. The occurrence of other operations in the frame is in accordance with the AFS algorithm, discussed in Section IV.

Estimation of PU Dynamics–Unpredictable PU dynamics result in intermittent connectivity and high channel switching rates for SUs. The observed correlations of PU activity over TVWS (demonstrated in [15]) permit us to estimate the PU profile based on past observations. This minimizes the time to identify an idle channel. Subsequently, incorporating the estimated PU profile while designing spectrum sensing sequences leads to increased discovery of spectrum opportunities [14]. In contrast, random scheduling of sensing events can lead to inefficient sensing, as SUs may end up sensing channels that are more likely to be busy. To account for PU dynamics, we employ an exponentially weighted moving average-based estimation approach, wherein the weight given to the recent sample is appropriately adjusted to cope with PU dynamics.

We assume that the MD has an initial estimate of the PU profile over all channels. Subsequent estimates are obtained through sensing. In our design, we use a sliding window of size T_{est} to estimate $T_{\text{on}}^{(i)}$ and $T_{\text{off}}^{(i)}$. These estimates, denoted by $\hat{T}_{\text{on}}^{(i)}$ and $\hat{T}_{\text{off}}^{(i)}$, respectively are used in computing the probability that channel i is idle at time t, denoted by $P_{\text{idle}}^{(i)}(t)$.

$$P_{\text{idle}}^{(i)}(t) = \frac{\hat{T}_{\text{off}}^{(i)}}{\hat{T}_{\text{off}}^{(i)} + \hat{T}_{\text{on}}^{(i)}} + \frac{\hat{T}_{\text{on}}^{(i)}}{\hat{T}_{\text{off}}^{(i)} + \hat{T}_{\text{on}}^{(i)}} \; e^{-\left(\frac{1}{\hat{T}_{\text{on}}^{(i)}} + \frac{1}{\hat{T}_{\text{off}}^{(i)}}\right)t}. \quad (1)$$

IV. Adaptive Frame Structure (AFS) Design

To reduce the control overhead, our protocol adaptively select one of four frame types: S, S/P-1, S/P-2, and D frames. The formats of these frame types are depicted in Fig. 2.

Four parameters determine the decision process of AFS design; $\hat{T}_{\text{off}}$, τ_c, L, and the arrival rate of new SU connection requests (τ_{new}). To simplify the notation, we drop the superscript i when we are not referring to any specific channel. Without loss of generality, we assume that each link transports only one flow at a time, which can be either HP or LP.

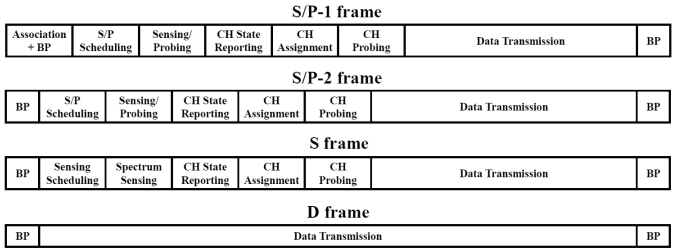

Fig. 2: Frame types used in AFS.

The rationale behind the design of AFS is as follows. If $\hat{T}_{\text{off}}^{(i)} > T_{\text{frame}}$ and $P_{\text{idle}}^{(i)}(t) > \beta$, where β is a design parameter, then channel i does not need to be sensed in the current frame, as this channel is expected to remain idle throughout the current frame. On similar grounds, if $\tau_c^{(i)} > T_{\text{frame}}$, then the quality of channel i is not expected to vary throughout the current frame duration, obviating the need to carry out channel probing. We interrupt the operation of the AFS algorithm every τ_{new} seconds to accommodate new traffic requests and to check for any changes in the rate demands of existing flows. This step is very crucial to cope with the dynamic nature of applications in today's mobile computing platforms (e.g., a user who subscribes to a VoD application can suddenly switch to an e-mail application, thereby changing his rate demand drastically). To jointly accommodate the arrival of new flows and changes in the rate demands of existing users, we use S/P-1 frame which enforces mandatory channel probing to obtain the link-dependent channel quality information.

To cope with PU dynamics and fluctuating channel quality, we use the S/P-2, S, and D frame types. The quantities whose values are not expected to expire within T_{frame} are termed *valid* entries. We continuously monitor the validity of each entry by using a timer at the MD. Initially, we group all channels for which $\tau_c \geq T_{\text{frame}}, \hat{T}_{\text{off}} \geq T_{\text{frame}}$, and $P_{\text{idle}}(t) > \beta$ into a list called List_1. Other channels that do not satisfy these conditions are grouped in List_2. If the channels in List_1 can guarantee the rate demands of all HP flows in $\mathcal{L}$, then we use a D frame, as we do not need to sense or probe any additional channels. The computation of the number of satisfied flows over a given channel set requires the knowledge of the channel quality, which varies from one link to another within the same network. On the other hand, LP flows can be transported over idle channels whose $\hat{T}_{\text{off}} > T_{\text{frame}}$, $P_{\text{idle}}(t) > \beta$ and $\tau_c \leq T_{\text{frame}}$. This way, we fully exploit the predicted values of PU usage profiles in minimizing the control overhead.

If the sum of the rate demands of HP flows cannot be satisfied by the channels in List_1, we defer from using a D frame. In this case, we first compute the maximum number of HP flows whose demands can be satisfied by the channels in List_1. Denote the set of links that transport these flows by $\mathcal{L}' \subseteq \mathcal{L}$. The objective now is to maximize the number of flows transported by the links in $\mathcal{L} \setminus \mathcal{L}'$, whose rate demands can be met by the channels in List_2 ($\text{List}_1 \cap \text{List}_2 = \emptyset$). By employing this methodology, we obviate the need to probe the channels in List_1, and meet the rate demands of flows carried by links in $\mathcal{L}'$ without incurring any additional overhead.

To minimize the control overhead, we check the validity of the coherence time τ_c for channels in List_2. Channels in List_2 that have a valid τ_c are grouped into a new list, called List_3. We check if the channels in List_3 can satisfy the rate demands of all flows transported by the links in $\mathcal{L} \setminus \mathcal{L}'$ (by solving Problem 1 in Section V-B). If so, we switch to an S frame, as we do not need to probe the channels in List_3 due to the validity of their channel quality information. If the demands of all flows transported over the links in $\mathcal{L} \setminus \mathcal{L}'$ cannot be satisfied, we switch to an S/P-2 frame. Before scheduling the sensing/probing processes, we determine the set of links whose demands can be met using List_3 channels. Denote this set by $\mathcal{L}''$, where $\mathcal{L}'' \subseteq \mathcal{L} \setminus \mathcal{L}'$. This way, we avoid the control overhead incurred by probing the channels whose τ_c is valid throughout T_{frame}. The remaining links in $\mathcal{L} \setminus \{\mathcal{L}', \mathcal{L}''\}$ are considered for the schedule of joint sensing and probing processes over the channels in List_2 with $\tau_c < T_{\text{frame}}$ and $\hat{T}_{\text{off}} > T_{\text{frame}}$ (we group these channels into a new list, called $\text{List}_4 \stackrel{\text{def}}{=} \text{List}_2 \setminus \text{List}_3$). It is to be instilled that if the receiver experiences any interference from a PU, the corresponding channel is reported to the MD during the next BP and not used again for data transmission until it is sensed to be idle, thereby restricting the maximum interference duration to T_{frame}. A pseudo-code of the AFS design is shown in Algorithm 1.

Algorithm 1 Adaptive Frame Structure Design

Input: $\hat{T}_{\text{on}}^{(i)}$, $\hat{T}_{\text{off}}^{(i)}$, $\tau_c^{(i)}$, $\mathcal{L}$, $R_d^{(j)}$, τ_{new}, T_{frame}, and β
Output: Frame type (S, D, S/P-1, or S/P-2)

Part I: Channels Categorization
for $i \in \mathcal{N}$ **do**
  if ($\tau_c^{(i)} > T_{\text{frame}}$ & $\hat{T}_{\text{off}}^{(i)} > T_{\text{frame}}$ & $P_{\text{idle}}^{(i)}(t) > \beta$) **then**
    add i to List_1
  else
    add i to List_2
  end if
end for
for $i \in \text{List}_2$ **do**
  if ($\tau_c^{(i)} > T_{\text{frame}}$ & $\hat{T}_{\text{off}}^{(i)} > T_{\text{frame}}$) **then**
    add i to List_3
  else if ($\hat{T}_{\text{off}}^{(i)} > T_{\text{frame}}$)
    add i to List_4
  end if
end for

Part II: Frame Type Selection
if (new links arrived or $R_d^{(j)}, j \in \mathcal{L}$, are updated) **then**
  set the frame type to S/P-1
else if (List_1 can support all HP flows in $\mathcal{L}$) **then**
  set the frame type to D
else if (Lists 1 & 3 can support all HP flows in $\mathcal{L}$) **then**
  set the frame type to S
else
  set the frame type to S/P-2
end if

Avoiding Stale Entries in the Database–A natural question that arises is what to be done with the links in $\mathcal{L}'$ during the

sensing/probing phase of S, S/P-1, and S/P-2 frames, and how can links in $\mathcal{L}' \cup \mathcal{L}''$ be better used during the probing operation of S/P-1 and S/P-2 frames. This issue arises because we wish to maintain synchronization among the associated links in the network, and improve the accuracy of estimated PU profiles by maximizing the number of sensing samples collected from a given channel per unit time.

Note that channels without a valid $\hat{T}_{\text{off}}$ entry are not considered for sensing/probing, which creates a "starvation" condition for these channels, i.e., such channels end up having an undetermined PU state even though they could exhibit good quality and/or low PU occupancy. To avoid this situation, we allow links in $\mathcal{L}'$ and links carrying LP flows to sense channels whose PU state is undetermined (List_4) along with channels in List_1 during the sensing phase of S frame, and allow links in $\mathcal{L}' \cup \mathcal{L}''$ along with links transporting LP flows to sense List_1, List_3, and List_4 channels during the sensing/probing phase of S/P-1 and S/P-2 frames. It is to be noted that no two links are made to sense the same channel at any given point in time, in order to increase the number of discovered opportunities. The scheduler implemented in QASPA excludes channels in List_1 and links in $\mathcal{L}'$. In turn, links in $\mathcal{L}'$ are made to sense maximum number of channels in List_1 and List_4 during the spectrum discovery period. Also, links contained in $\mathcal{L}''$ are made to sense channels in List_3, during the spectrum discovery phase of S/P-1 and S/P-2 frames. After sensing the scheduled channels in List_3, links contained in $\mathcal{L}''$ use the remaining time in the discovery phase (if any) to sense additional channels in List_4 in an attempt to improve the overall discovery efficiency.

V. QASPA Design

To maximize the sensing efficiency, QASPA encompasses two functional blocks: an adaptive double-threshold-based sensing mechanism and a parallel sensing/probing scheduling mechanism.

A. Optimal Adaptive Double-threshold-based Sensing Algorithm

In QASPA, we resort to a double-threshold-based sensing (DTS) approach instead of the conventional single-threshold sensing (STS). As will be shown in this section, while achieving the same sensing accuracy, DTS consumes several orders of magnitude less sensing time than STS. Fig. 3 depicts STS as well as DTS. DTS uses two thresholds (ϵ_l and ϵ_h) in contrast to only one threshold (ϵ) in STS. In DTS, the sensed channel is considered idle if the received energy over this channel is below ϵ_l, busy if the received energy exceeds ϵ_h, and uncertain if the received energy falls between ϵ_l and ϵ_h.

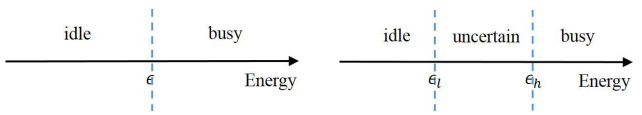

(a) Single-threshold (STS) (b) Double-threshold (DTS)

Fig. 3: Single- and double-threshold sensing approaches.

In principle, the spectrum sensing accuracy is characterized by the probabilities of miss-detection and false-alarm, denoted by P_{md} and P_{fa}, respectively. For a given sensing threshold ϵ, $P_d \triangleq 1 - P_{md}$ and P_{fa} can be expressed as [17]:

$$P_d = Q\left(\left(\frac{\epsilon}{\sigma_n^2} - \gamma - 1\right)\sqrt{\frac{U}{2\gamma+1}}\right) \quad (2)$$

$$P_{fa} = Q\left(\left(\frac{\epsilon}{\sigma_n^2} - 1\right)\sqrt{U}\right) \quad (3)$$

where $Q(\cdot)$ is the complementary distribution function of a standard Gaussian random variable, γ is the SNR of the received PU signal, U is the number of sensing samples ($U = \tau_s f_s$, where f_s is the sampling frequency), and σ_n^2 is the variance of the additive white Gaussian noise.

Using moderate sensing durations, STS cannot simultaneously achieve low P_{md} and low P_{fa}, as shown in Fig. 4. In Fig. 4, $P(E|H_1)$ is the probability density function (pdf) of the received energy given that the channel is busy, and $P(E|H_0)$ is the pdf of the received energy given that the channel is idle. Fig. 4(a) shows that for a moderate sensing duration, and hence a moderate variance of the random variable E, STS cannot simultaneously guarantee low P_{md} and low P_{fa}. Reducing the threshold ϵ reduces P_{md}, but due to the direct relationship between P_{md} and P_{fa}, P_{fa} increases. On the other hand, increasing the sensing duration (and hence reducing the variance of E) increases the possibility of simultaneously satisfying the required P_{md} and P_{fa}, as shown in Fig. 4(b), but this is undesirable as we intend to minimize the time spent in the discovery phase. Accordingly, we resort to a DTS scheme, as shown in Fig. 4(c). DTS can simultaneously achieve low P_{md} and low P_{fa} using a much smaller sensing time than STS. In DTS, ϵ_l is selected such that the required P_{md} (which equals to $1 - \bar{P}_d$) is satisfied. On the other hand, ϵ_h is selected to satisfy the required P_{fa} (which equals to $\bar{P}_{fa}$). The relations between ϵ_l and $\bar{P}_d$, and ϵ_h and $\bar{P}_{fa}$ are given by:

$$\epsilon_l(\tau_s, \bar{P}_d) = \sigma_n^2\left[\sqrt{\frac{2\gamma+1}{U}}Q^{-1}(\bar{P}_d) + \gamma + 1\right] \quad (4)$$

$$\epsilon_h(\tau_s, \bar{P}_{fa}) = \sigma_n^2\left[\sqrt{\frac{1}{U}}Q^{-1}(\bar{P}_{fa}) + 1\right]. \quad (5)$$

The required sensing time to satisfy $\bar{P}_d$ and $\bar{P}_{fa}$ for STS and DTS schemes, denoted by $\tau_{s,\text{single}}$ and $\tau_{s,\text{double}}$, respectively, can be easily expressed as [17]:

$$\tau_{s,\text{single}} = \frac{1}{\gamma^2 f_s}\left[Q^{-1}(\bar{P}_{fa}) - Q^{-1}(\bar{P}_d)\sqrt{2\gamma+1}\right]^2 \quad (6)$$

$$\tau_{s,\text{double}} = \frac{1}{f_s}\left[\frac{\epsilon_h\sqrt{2\gamma+1}Q^{-1}(\bar{P}_d) - \epsilon_l Q^{-1}(\bar{P}_{fa})}{\epsilon_l - \epsilon_h(\gamma+1)}\right]^2 \quad (7)$$

Let ρ denote the probability of uncertainty (i.e., the probability that the received energy over a given channel falls between ϵ_l and ϵ_h). Fig. 5 compares $\tau_{s,\text{single}}$ and $\tau_{s,\text{double}}$ for different $\bar{P}_d$ and $\bar{P}_{fa}$ values. It shows that for a given $\bar{P}_d$ and $\bar{P}_{fa}$, and with a small value of ρ, $\tau_{s,\text{double}}$ is 3 to 4 orders of magnitude

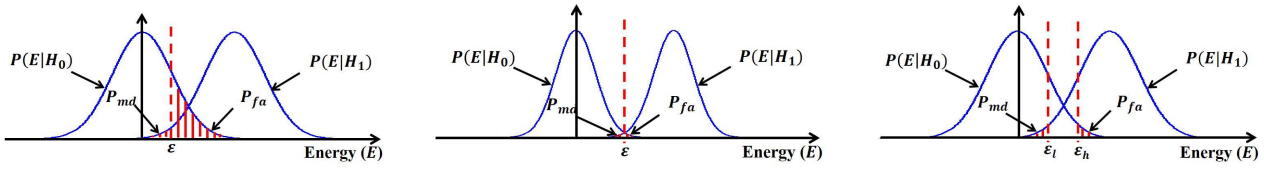

(a) STS with a moderate sensing duration (b) STS with a long sensing duration (c) DTS

Fig. 4: Single-threshold vs. double-threshold sensing.

less than $\tau_{s,\text{single}}$.

In spite of achieving much smaller sensing time than STS, DTS faces the problem of the uncertain region. DTS can certainly (i.e., while satisfying $\bar{P}_d$ and $\bar{P}_{fa}$) determine the state of the channel only if its received energy is below ϵ_l or above ϵ_h. Otherwise, the state of the channel cannot be determined certainly. To overcome this problem, we propose in this paper an adaptive DTS-based (ADTS) algorithm.

The idea behind the ADTS algorithm comes from equations (4) and (5). For a fixed $\bar{P}_d$ and $\bar{P}_{fa}$, if the sensing time increases (hence, $U = \tau_s f_s$ increases) ϵ_l increases and ϵ_h decreases, which causes ρ to decrease. Therefore, starting with a reasonable value of U, if the sensing outcome is uncertain, gradually increasing U may eventually result in having a certain outcome. However, since the total sensing time in each frame cannot exceed $T_{s,\max}$ (obtained from the sensing-throughput tradeoff. See, for example, [17]), and each link is required to sense a certain number of channels (M_j for link $j \in \mathcal{L}$), the sensing time of a channel over link j cannot exceed $T_{s,\max}/M_j$. Therefore, starting with a given U that resulted in uncertain channel state, gradually increasing U may not lead to a certain outcome before reaching the maximum value of U. Accordingly, instead of increasing U, it might be better (under certain conditions) to stop sensing the current channel and use the saved sensing time for sensing the next channel(s).

We formulate the optimal ADTS problem as an optimal stopping rule with horizon $a \stackrel{\text{def}}{=} \tau_{s,\max}/\delta$, where $\tau_{s,\max}$ is the maximum allocated sensing time for the given channel and δ is the value of the sensing time increment. An optimal stopping problem with horizon a is defined by two components [11]:

- A sequence of random variables, X_1, X_2, ..., X_a, whose joint distribution is assumed to be known.
- A sequence of real-valued reward functions, $y_0, y_1(x_1)$, $y_2(x_1, x_2), \ldots, y_a(x_1, x_2, \ldots, x_a)$.

In our formulation, $X_i, i = 1, \ldots, a$, is defined as the state of the sensed channel at the end of the ith sensing slot. X_i equals 1 if the state is idle, -1 if it is busy, and 0 if it is uncertain. The distribution of X_i is given by: $P_{1,i} \stackrel{\text{def}}{=} \Pr\{X_i = 1\} = \Pr\{E_i \leq \epsilon_{l,i}\}$, $P_{-1,i} \stackrel{\text{def}}{=} \Pr\{X_i = -1\} = \Pr\{E_i \geq \epsilon_{h,i}\}$, and $P_{0,i} \stackrel{\text{def}}{=} \Pr\{X_i = 0\} = \Pr\{\epsilon_{l,i} < E_i < \epsilon_{h,i}\}$, where E_i is the output of the energy detector at the end of the ith slot, and $\epsilon_{l,i}$ and $\epsilon_{h,i}$ are the values of ϵ_l and ϵ_h at the ith slot, respectively. As mentioned before, for any i and j such that $i > j$, $\epsilon_{l,i} > \epsilon_{l,j}$ and $\epsilon_{h,i} < \epsilon_{h,j}$. E_i is assumed to follow a central (noncentral) Chi-square distribution in the absence (presence) of the PU signal, with U_i degrees of freedom [18].

Consider the jth sensed channel in a frame, the reward of stopping at the end of the ith sensing slot, $y_i(x_1, \ldots, x_i)$, depends only on x_i and is defined as follows. Irrespective of the value of x_i, stop sensing at the end of the ith slot will save $(a - i)\delta$ seconds, which can then be used in sensing the $j + 1$st channel in the frame (as explained later in this section). If $x_i = 0$, then stop sensing will waste $i\delta$ seconds consumed in sensing the jth channel without concluding its state. We associate with each channel a quality metric, denoted by q_j for the jth sensed channel. Channels are sensed based on their qualities such that the best channel is sensed first (i.e., $q_j > q_{j+1}, \forall j$). q_j is defined as a linear combination of P_{idle} and the normalized expected rate of the channel. Therefore, $y_i(x_1, \ldots, x_i) = y_i(x_i)$ can be expressed as (with $y_0 = 0$):

$$\begin{aligned} y_i(x_1, \ldots, x_i) &= y_i(x_i) \\ &= \begin{cases} (a-i)\delta q_{j+1}, & \text{if } x_i = \pm 1 \\ (a-i)\delta q_{j+1} - i\delta q_j, & \text{if } x_i = 0 \end{cases} \\ &= (a-i)\delta q_{j+1} - (1 - |x_i|)\, i\delta q_j. \end{aligned} \tag{8}$$

Recall that our objective is to obtain the state of the sensed channel while satisfying $\bar{P}_d$ and $\bar{P}_{fa}$. Hence, if $x_i = \pm 1$ we stop sensing. The optimal decision to stop or continue sensing is only taken when $x_i = 0$. When $x_i = 0$, stop sensing will cause losing $i\delta q_j$, whereas continue sensing will either result in returning $i\delta q_j$ but losing δq_{j+1} (if $x_{i+1} = \pm 1$) or losing an additional δq_j (if $x_{i+1} = 0$).

Let $V_i^{(a)}(x_1, \ldots, x_i)$ be the maximum return that can be obtained starting from stage i having observed $X_1 = x_1$, ..., $X_i = x_i$. Then, $V_i^{(a)}(x_1, \ldots, x_i) = V_i^{(a)}(x_i)$ is given by:

$$\begin{aligned} V_i^{(a)}(x_1, \ldots, x_i) &= V_i^{(a)}(x_i) \\ &= \max\left\{ y_i(x_i), \mathbb{E}\left[V_{i+1}^{(a)}(X_{i+1}) | X_1 = x_1, \ldots, X_i = x_i \right] \right\}. \end{aligned} \tag{9}$$

Therefore, it is optimal to stop sensing at the end of the ith slot if $V_i^{(a)}(x_i) = y_i(x_i)$, otherwise it is optimal to continue sensing. Note that $V_a^{(a)}(x_a) = y_a(x_a)$. The value of the stopping rule problem is given by $V_0^{(a)}$. Accordingly, the optimal stopping sensing problem can be written as follows:

Problem 1:

$$V_0^{(a)} = \underset{j \in \{1,2,\ldots,a\}}{\text{maximize}}\ \mathbb{E}\left[V_1^{(a)}(X_1) \right] \tag{10}$$

$$\text{subject to:}\quad j \leq (1 - |x_i|)\, a + |x_i| i, \forall i \in \{1, 2, \ldots, a\}. \tag{11}$$

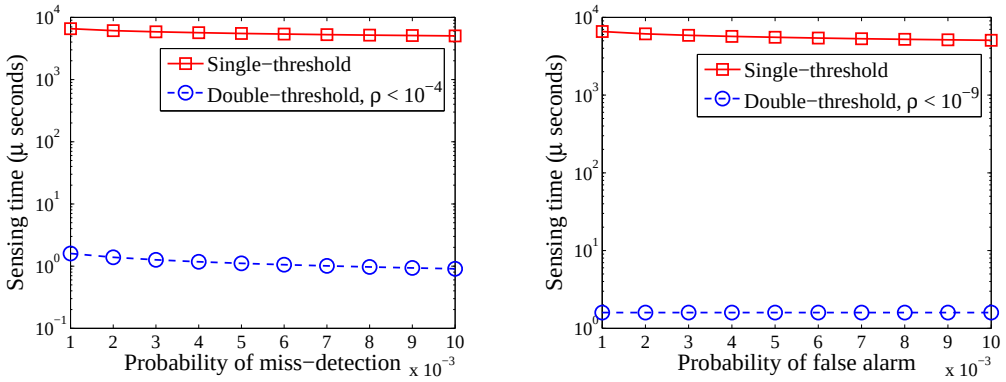

(a) $P_{fa} = 0.001$ (b) $P_d = 0.999$

Fig. 5: Sensing time vs. (a) P_{md} and (b) P_{fa} ($P_{\text{idle}} = 0.5$, $f_s = 6$ MHz, and $\gamma = -15$ dB).

Recall that the objective function value $V_0^{(a)}$ is given by $\max\left\{y_0, \mathbb{E}\left[V_1^{(a)}(X_1)\right]\right\}$ and $y_0 = 0$. Constraint 11 ensures that a link will stop sensing a given channel once the sensing outcome of that channel is certain (i.e., $x_i = \pm 1$). So, if $|x_i| = \pm 1$, then the stopping time j needs to be less than or equal to i. If $x_i = 0$, constraint 11 reduces to $j \leq a$, which is redundant.

Because we need to stop sensing at slot a, using (9) we can obtain the optimal rule at slot $a-1$. Then, knowing the optimal rule at slot $a-1$, we can derive the optimal rule at slot $a-2$, and so on back to slot 1. To make this backward induction procedure clearer, we show the analysis of the first few steps. Consider slot $a-1$,

$$V_{a-1}^{(a)}(x_{a-1}) = \max\Big\{y_{a-1}(x_{a-1}), \mathbb{E}[V_a^{(a)}(X_a)|X_1 = x_1, \ldots, X_{a-1} = x_{a-1}]\Big\}. \tag{12}$$

However, $\mathbb{E}[V_a^{(a)}(X_a)|X_1 = x_1, \ldots, X_{a-1} = x_{a-1}] = \mathbb{E}[y_a(x_a)|X_1 = x_1, \ldots, X_{a-1} = x_{a-1}] = \mathbb{E}[y_a(x_a)] = -P_{0,a-1}a\delta q_j$. Therefore,

$$V_{a-1}^{(a)}(x_{a-1}) = \max\Big\{\delta q_{j+1} - (a-1)\delta q_j, -P_{0,a-1}a\delta q_j\Big\}. \tag{13}$$

Hence, it is optimal to stop sensing at the end of slot $a-1$ if the following condition in (14) is satisfied. Otherwise, it is optimal to continue sensing.

$$P_{0,a-1} > -\left(\frac{q_{j+1}}{q_j} - (a-1)\right)/a. \tag{14}$$

Similarly, if (14) is satisfied, then

$$V_{a-2}^{(a)}(x_{a-2}) = \max\Big\{2\delta q_{j+1} - (a-2)\delta q_j, \delta q_{j+1} + P_{0,a-2}\delta q_j(1-a)\Big\}. \tag{15}$$

In this case, it is optimal to stop at $a-2$ if $P_{0,a-2} > \left(\frac{q_{j+1}}{q_j} - (a-2)\right)/(1-a)$.

The backward induction procedure continues in the same way as above. Next, we describe our proposed algorithm for adaptively adjusting the sensing time and accordingly adjusting ϵ_l and ϵ_h can be described as follows. Consider the jth link in the network, the maximum sensing time allocated for each channel is set initially to $T_{s,\max}/M_j$. Our adaptive sensing algorithm takes M_j rounds. During each round, only one channel is sensed (we index the channel sensed during the kth round by k, and denote its sensing time by τ_{s_k}). In each round, after sensing the corresponding channel, the maximum sensing time allocated for the next channel is updated. We denote the maximum sensing time allocated for channel i during the kth round by $\tau_{s_i,\max}^{(k)}$. A pseudo-code of our optimal adaptive sensing mechanism (as executed by link j) is shown in Algorithm 2.

Algorithm 2 Optimal Adaptive Double-threshold-based Sensing Algorithm

Input: $T_{s,\max}$, M_j, δ, and c
Output: $\tau_{s_k}, k \in \mathcal{M}_j = \{1, 2, \ldots, M_j\}$
1: Set the maximum sensing time per channel to $T_{s,\max}/M_j$ (i.e., $\tau_{s_i,\max} = T_{s,\max}/M_j, \forall i \in \mathcal{M}_j$)
2: **for** $i \in \mathcal{M}_j$ **do**
3: Set the sensing time, τ_{s_i}, to $c\,\delta$
4: Compute the corresponding ϵ_l and ϵ_h from (4) and (5)
5: Sense the channel for τ_{s_i} seconds
6: **while** the state of the channel is uncertain and $\tau_{s_i} < \tau_{s_i,\max}$ **do**
7: Use (9) to determine the optimal decision
8: **if** the optimal decision is to continue sensing **then**
9: $\tau_{s_i} = \tau_{s_i} + \delta$
10: Go to line 4
11: **else**
12: Go to line 15
13: **end if**
14: **end while**
15: **if** $i < M_j$ **then**
16: $\tau_{s_{i+1},\max} = \tau_{s_{i+1},\max} + (\tau_{s_i,\max} - \tau_{s_i})$
17: **end if**
18: **end for**

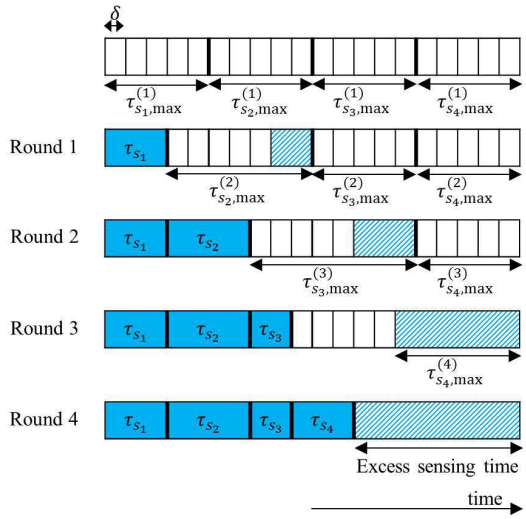

Fig. 6: An illustrative example for the adaptive sensing algorithm.

Fig. 6 shows an illustrative example for the adaptive sensing algorithm, where the number of channels to be sensed is 4. Initially, each channel is allocated a maximum sensing time of $T_{s,\max}/4$, which is assumed in this example to be equal to 5δ. The first channel is sensed in the first round and its sensing time τ_{s_1} is determined according to the above algorithm. In our example, τ_{s_1} is assumed to be 3δ (i.e., 2δ less than the maximum allocated sensing time). The saved 2δ seconds are allocated for the next channel, so that the maximum sensing time for the second channel becomes $5\delta + 2\delta = 7\delta$. The remaining three rounds continue in the same way.

Remark 1: In the above formulation of the optimal ADTS scheme (Problem 1), we require a link to stop sensing a given channel once the state of this channel is certain (i.e., idle or busy while satisfying the required P_{md} and P_{fa}). Our objective in Problem 1 is to minimize the per-channel sensing time (and hence maximize the total number of sensed channels) subject to satisfying the required P_{md} and P_{fa}.

Another ADTS scheme can be formulated by incorporating P_{md} and P_{fa} into the optimization objective (in addition to the constraints). In this case, the objective is to maximize the total number of sensed channels that result in a certain outcome (hence, satisfy the minimum requirements on P_{md} and P_{fa}) as well as minimize P_{md} and P_{fa}. Therefore, even if the sensing outcome of a given channel at the end of the ith slot is certain (i.e., $x_i = \pm 1$), a link may decide to continue sensing this particular channel; because this will improve its sensing accuracy (i.e., achieve lower values of P_{md} and P_{fa}). We refer to this version of the ADTS scheme as optimal ADTS with enhanced accuracy (ADTSEA). The optimal ADTSEA can be formulated by modifying the stopping reward in (8) as follows:

$$y_i(x_1,\ldots,x_i) = y_i(x_i) = \begin{cases} (a-i)\delta q_{j+1} + (1-P_{md})(1-P_{fa}), & \text{if } x_i = \pm 1 \\ (a-i)\delta q_{j+1} - i\delta q_j, & \text{if } x_i = 0. \end{cases} \tag{16}$$

Consider the case when $x_i = \pm 1$. Note from (16) that although the first term in $y_i(x_i)$ decreases with i, the second term increases with i (both P_{md} and P_{fa} decrease with the sensing time). Because in optimal ADTSEA a link might continue sensing a given channel after its state being certain, constraint (11) in Problem 1 is removed in the case of ADTSEA.

In our current framework, we aim to maximize the amount of discovered opportunities subject to stringent requirements on PU protection, rather than optimizing the sensing accuracy. Therefore, in this paper we focus on the optimal ADTS scheme.

B. Scheduling of Sensing/Probing Processes for HP Flows

In [2], an access point and spectral band selection scheme, called MAWS, is proposed. In this scheme, the channel quality is inferred by periodically probing random spectral bands without any proper scheduling mechanism. However, in our scheme, while scheduling the sensing/probing processes for links transporting HP flows, we probabilistically guarantee the aggregate bandwidth of the discovered opportunities by each link j to be equal to $R_d^{(j)} + \kappa$, where $\kappa < R_d^{(j)}$. The rationale behind this approach is two-fold; to include the impact of fluctuations in channel quality, and to ensure serving the links that carry LP flows in the network using the excess discovered opportunities. Although the effect of mobility is indirectly being captured through the coherence time, it is very hard to guarantee the validity of the estimated channel quality with lapse in time. We assume that this quality does not vary drastically in a short interval of time. Hence, for any link j with rate demand $R_d^{(j)}$, we choose κ such that $\kappa < R_d^{(j)}$.

We formulate our scheduling problem as a constrained optimization problem with the objective of maximizing the number of HP flows with satisfied rate demands. Let $\tilde{\mathcal{N}}$ ($|\tilde{\mathcal{N}}| = \tilde{N}$) be the set of channels that are considered for sensing/probing scheduling, and let $\tilde{\mathcal{L}}$ ($|\tilde{\mathcal{L}}| = \tilde{L}$) be the set of links that will participate in the sensing/probing process. Let $y_i^{(j)}, i \in \tilde{\mathcal{N}}, j \in \tilde{\mathcal{L}}$, be a binary variable which equals 1 if channel i is scheduled to be sensed/probed by link j, and 0 otherwise. Let $R_i^{(j)}$ be the rate supported by channel i over link j, and $\Theta_i^{(j)} \overset{\text{def}}{=} y_i^{(j)} R_i^{(j)} P_{\text{idle}}^{(i)}(t)$. Then, our optimization problem can be formulated as a non-linear binary program as follows:

Problem 2:

$$\underset{\substack{y_i^{(j)} \\ i\in\tilde{\mathcal{N}}, j\in\tilde{\mathcal{L}}}}{\text{maximize}} \left\{ \sum_{j\in\tilde{\mathcal{L}}} \mathbf{1}_{\left\{\sum_{i\in\tilde{\mathcal{N}}} \Theta_i^{(j)} > R_d^{(j)} + \kappa\right\}} + \frac{\sum_{i\in\tilde{\mathcal{N}}} \sum_{j\in\tilde{\mathcal{L}}} y_i^{(j)} R_i^{(j)}}{\sum_{i\in\tilde{\mathcal{N}}} \sum_{j\in\tilde{\mathcal{L}}} y_i^{(j)} R_{\max}} \right\} \tag{17}$$

$$\text{subject to:} \quad \sum_{j\in\tilde{\mathcal{L}}} y_i^{(j)} \leq 1, \forall i \in \tilde{\mathcal{N}} \tag{18}$$

$$\sum_{i\in\tilde{\mathcal{N}}} y_i^{(j)} \leq M_j, \forall j \in \tilde{\mathcal{L}} \tag{19}$$

where $R_{\max}$ is the maximum supported data rate by any channel $i \in \tilde{\mathcal{N}}$, and $\mathbf{1}_{\{\cdot\}}$ is the indicator function. The first term in the objective function indicates that we wish to maximize the number of satisfied HP flows through parallel sensing/probing. The second term is intended to resolve the tie in case of multiple optimal solutions. The second term always has a value ≤ 1. Constraint (18) ensures that no channel can be sensed/probed by more than one link in a given frame. Constraint (19) restricts the maximum number of channels that can be sensed/probed by link j to a predefined value M_j. Inoperable links whose requested rate demands cannot be met are made to sense the channels whose PU state is undetermined to prevent the occurrence of a "starvation" condition. Constraints (18) and (19) can be written in matrix form as $A\vec{y} \leq \vec{b}$, where $A = (a_{ij})_{1\leq i\leq \tilde{N}+\tilde{L}, 1\leq j\leq \tilde{N}\tilde{L}}$, $\vec{y} = (y_i^{(j)})_{i\in\tilde{\mathcal{N}}, j\in\tilde{\mathcal{L}}}$, and $\vec{b} = (1, \ldots, 1, M_1, \ldots, M_{\tilde{L}})^T \in \mathbb{R}_{\tilde{N}+\tilde{L}}$.

Proposition 1. Matrix A in Problem 2 is totally unimodular (TU) [19]. This means that the decision variables $y_i^{(j)}$ can be relaxed to continuous variables, and the resulted solution to Problem 2 is still optimal.

Proof: It can be seen that: (i) $a_{ij} \in \{0, 1\}$, (ii) each column in A contains at most two nonzero coefficients (i.e., $\sum_{i=1}^{\tilde{N}+\tilde{L}} |a_{ij}| \leq 2$), and (iii) there exists a partition ($M_1 = \{1, \ldots, \tilde{N}\}, M_2 = \{\tilde{N}+1, \ldots, \tilde{N}+\tilde{L}\}$) of rows such that each column j containing two nonzero coefficients satisfies: $\sum_{i\in M_1} a_{ij} - \sum_{i\in M_2} a_{ij} = 0$. Since the above three conditions are satisfied, matrix A is TU [19]. ■

C. Sensing/Probing Scheduling with Additional Practical Constraints

In existing channel aggregation systems, a device cannot aggregate two channels if the frequency separation between these channels exceeds a certain threshold. In this section, we modify the sensing/probing scheduling scheme formulated in Problem 2 to account for this additional hardware constraint.

The channel aggregation constraint can be stated as follows: $\forall l, k \in \tilde{\mathcal{N}}$ and $\forall j \in \tilde{\mathcal{L}}$, if $|l-k| > \mathcal{B}$ then $y_l^{(j)} + y_k^{(j)} \leq 1$, where $\mathcal{B}$ is the maximum allowable separation between the aggregated frequency channels. To formally write this constraint, we introduce the following binary variables:

$$\begin{aligned} d_{l,k} &= \begin{cases} 1, & \text{if } |l-k| > \mathcal{B} \\ 0, & \text{otherwise} \end{cases}, \forall l, k \in \tilde{\mathcal{N}}, \forall j \in \tilde{\mathcal{L}} \\ e_{l,k}^{(j)} &= \begin{cases} 1, & \text{if } y_l^{(j)} + y_k^{(j)} \leq 1 \\ 0, & \text{otherwise} \end{cases}, \forall l, k \in \tilde{\mathcal{N}}, \forall j \in \tilde{\mathcal{L}}. \end{aligned} \tag{20}$$

Then, the constraint can be written as $d_{l,k} \leq e_{l,k}^{(j)}, \forall l, k \in \tilde{\mathcal{N}}, \forall j \in \tilde{\mathcal{L}}$. Next, we present a simplified way of representing the binary variables in (20).

1. $d_{l,k} = 1$ iff $|l-k| > \mathcal{B}$ can be reformulated as follows:
   - if $|l-k| > \mathcal{B}$ then $d_{l,k} = 1$ can be equivalently written as $|l-k| - (M+1)\, d_{l,k} \leq \mathcal{B} - 1$, where M is an upper bound of $|l-k| - \mathcal{B}$.
   - if $d_{l,k} = 1$ then $|l-k| > \mathcal{B}$ can be equivalently written as $|l-k| + m d_{l,k} \geq m + \mathcal{B}$, where m is a lower bound of $|l-k| - \mathcal{B}$.

   Because $1 \leq |l-k| \leq \tilde{N}$, we set M and m to $\tilde{N} - \mathcal{B}$ and $1 - \mathcal{B}$, respectively. Hence, '$d_{l,k} = 1$ iff $|l-k| > \mathcal{B}$' can be equivalently written as: $(\mathcal{B}-1)\, d_{l,k} + 1 \leq |l-k| \leq \left(\tilde{N} - \mathcal{B} + 1\right) d_{l,k} + \mathcal{B} - 1$.
2. Similar to point 1 above, $e_{l,k}^{(j)} = 1$ iff $y_l^{(j)} + y_k^{(j)} \leq 1$ can be reformulated as follows:
   - if $y_l^{(j)} + y_k^{(j)} \leq 1$ then $e_{l,k}^{(j)} = 1$ can be equivalently written as $2 - y_l^{(j)} - y_k^{(j)} \leq 2e_{l,k}^{(j)}$.
   - if $e_{l,k}^{(j)} = 1$ then $y_l^{(j)} + y_k^{(j)} \leq 1$ can be equivalently written as $2 - y_l^{(j)} - y_k^{(j)} \geq e_{l,k}^{(j)}$.

   Hence, '$e_{l,k}^{(j)} = 1$ iff $y_l^{(j)} + y_k^{(j)} \leq 1$' can be equivalently written as: $e_{l,k}^{(j)} \leq 2 - y_l^{(j)} - y_k^{(j)} \leq 2e_{l,k}^{(j)}$.

Accordingly, to account for the additional channel aggregation constraint, we add the following constraints to Problem 2:

$$\begin{aligned} (\mathcal{B}-1)d_{l,k} + 1 &\leq |l-k| \\ &\leq \left(\tilde{N} - \mathcal{B} + 1\right) d_{l,k} + \mathcal{B} - 1, \forall l, k \in \tilde{\mathcal{N}} \end{aligned} \tag{21}$$

$$e_{l,k}^{(j)} \leq 2 - y_l^{(j)} - y_k^{(j)} \leq 2e_{l,k}^{(j)}, \forall l, k \in \tilde{\mathcal{N}}, \forall j \in \tilde{\mathcal{L}} \tag{22}$$

$$d_{l,k} \leq e_{l,k}^{(j)}, \forall l, k \in \tilde{\mathcal{N}}, \forall j \in \tilde{\mathcal{L}} \tag{23}$$

$$d_{l,k}, e_{l,k}^{(j)} \in \{0, 1\}, \forall l, k \in \tilde{\mathcal{N}}, \forall j \in \tilde{\mathcal{L}}. \tag{24}$$

VI. Allocation of Data Channels

In this section, we propose an efficient data channel assignment algorithm, which incorporates channel aggregation and bonding techniques. Our objective is to minimize the number of channels allocated to any HP link, in an attempt to maximize the number of admitted flows in the network.

A. Channel Assignment Algorithm

Several wireless protocol designs have been proposed to improve the spatial reuse of the network (e.g., [6]–[8]). In addition to maximize the network's spatial reuse, our problem is further complicated by the need to meet the rate demands of the HP flows and guarantee interference-free communication for PUs. The proposed channel assignment algorithm attempts to overcome these challenges by exploiting the available resources (channels) to the maximum extent.

Given the sensing/probing outcomes provided by the active links, the MD initially computes the feasibility of supporting the rate demands of each HP flow using the channels which were sensed to be idle by the corresponding link. Let $\mathcal{K}_j$ ($|\mathcal{K}_j| = K_j$) be the set of idle channels discovered by link

j. The MD checks if $\sum_{i=1}^{K_j} R_i^{(j)} > R_d^{(j)}$. If this condition is satisfied, the MD executes Problem 3 below to compute the optimal number of channels needed to support the rate demand on that link. The links that do not meet the above condition are classified as unsatisfied links. Let $x_i^{(j)}, i \in \mathcal{K}_j$, be a binary variable which equals 1 if channel i is assigned to link j, and 0 otherwise. Our optimization problem is stated as follows.

Problem 3:

$$\underset{x_i^{(j)}, i \in \mathcal{K}_j}{\text{minimize}} \left\{ \sum_{i \in \mathcal{K}_j} x_i^{(j)} + \frac{\sum_{i \in \mathcal{K}_j} x_i^{(j)} R_i^{(j)}}{\sum_{i \in \mathcal{K}_j} x_i^{(j)} R_{\max}} \right\} \tag{25}$$

$$\text{subject to:} \quad \sum_{i \in \mathcal{K}_j} x_i^{(j)} R_i^{(j)} \geq R_d^{(j)}. \tag{26}$$

Problem 3 is a non-linear binary program. The objective function aims at minimizing the number of channels to be allocated for a given link while meeting the requested rate demand. The second term in the objective function is used to break the ties among multiple optimal solutions. When multiple optimal solutions exist, our formulation ensures the selection of channels with minimum aggregated data rate, such that the remaining channel(s) can be used during the second round of channel probing to support other unsatisfied links in the network.

B. Channel Assignment Algorithm with Additional Practical Constraints

In this section, we modify the channel assignment scheme formulated in Problem 3 to account for two additional constraints: (i) a link cannot aggregate two channels if the frequency separation between these channels exceeds $\mathcal{B}$, and (ii) it cannot bond/aggregate more than $\mathcal{C}$ channels. Similar to Section V-C, to meet the first requirement we add the following constraints to Problem 3:

$$\begin{aligned}(\mathcal{B}-1)w_{l,k} + 1 &\leq |l-k| \\ &\leq (K_j - \mathcal{B} + 1)\, w_{l,k} + \mathcal{B} - 1, \forall l, k \in \mathcal{K}_j\end{aligned} \tag{27}$$

$$v_{l,k}^{(j)} \leq 2 - x_l^{(j)} - x_k^{(j)} \leq 2v_{l,k}^{(j)}, \forall l, k \in \mathcal{K}_j \tag{28}$$

$$w_{l,k} \leq v_{l,k}^{(j)}, \forall l, k \in \mathcal{K}_j \tag{29}$$

$$w_{l,k}, v_{l,k}^{(j)} \in \{0, 1\}, \forall l, k \in \mathcal{K}_j. \tag{30}$$

To meet the second requirement, we add the following constraint to Problem 3:

$$\sum_{i \in \mathcal{K}_j} x_i^{(j)} \leq \mathcal{C}. \tag{31}$$

C. Second Round of Channel Probing

To meet the rate demand of an unsatisfied link, we first compute the maximum data rate that can be supported by its channel set, i.e., the channels that were sensed/probed by that link. Consequently, we schedule this link for a second round of probing over the channels that have been deemed excess by the satisfied links in the network. More specifically, we allocate a total of 3 MASs before the start of a data transmission in S, S/P-1, and S/P-2 frames for the second round probing, wherein a maximum of one channel can be probed by any unsatisfied link in the network. If the rate demand of the HP flow can be satisfied by combining the channels in its own channel set and the newly probed channel, the receiver sends a positive feedback to the transmitter, after which the transmitter starts sending data by aggregating/bonding these channels.

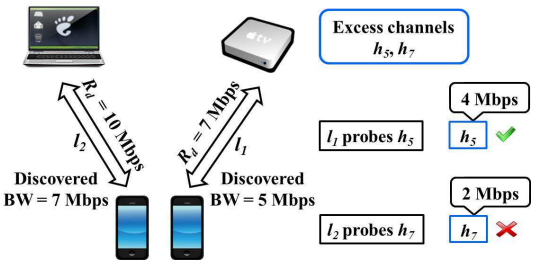

Fig. 7: Example illustrating the second round probing process.

In our design, we assume the presence of several links carrying LP flows throughout the operation of the network. We are interested in supporting LP alongside HP flows. The drastic increase in the number of discovered opportunities brought in by QASPA always guarantees fair share of bandwidth for the LP flows. Note that, LP flows have no stringent bandwidth requirement, which permits us to assign channels to these flows regardless of their exhibited quality. The idle channels which are not assigned to HP flows are used by LP flows.

As an example for the second round probing, consider two links l_1 and l_2 with rate demands of 10 and 7 Mbps, respectively, as illustrated in Fig. 7. Assume that the amount of bandwidth discovered by these two links during their sensing/probing phase are 7 and 5 Mbps, respectively. Hence, their rate demands were not met using the discovered opportunities, making these links inoperable. Assume that h_5 and h_7 are the channels that have been deemed excess by the satisfied links in the network. We randomly assign h_5 to l_1 and h_7 to l_2 for probing. We allocate channels in a random fashion because we do not know the link-dependent channel quality information ahead of time. Assume that h_5 can support 4 Mbps over l_1 and h_7 can support 2 Mbps over l_2. Hence, we are able to satisfy the rate demand of l_1, whereas the rate demand of l_2 remains unsatisfied. This way, we are able to increase the number of satisfied links at the cost of second round of probing.

Next, we discuss two important aspects in our protocol: the control channel selection, and the adaptive reporting strategy.

Common Control Channel (CCC) Selection–The dependance on a dedicated CCC for control packets exchange has been an impending issue since the inception of CRNs. Unlike ISM bands, TVWS communication demands guarantee on interference-free communication for the PUs. This requirement curbs the use of any channel in the licensed TVWS for communicating control/management information without the knowledge of its current state (idle/busy). The other issue in maintaining a network-wide CCC in a multi-channel system is synchronization (i.e., all SUs need to rendezvous during

the time of control packets exchange), which requires an appropriate signaling mechanism. By exploiting the properties of quorum systems, several distributed rendezvous schemes have been proposed in the literature (see, for example, [20]–[24] and references therein).

In here, we exploit the centralized architecture to maintain a time-varying CCC using the estimated PU profiles. The selection of a channel as a CCC depends on its PU state rather than its quality, as control packets are transmitted at the lowest rate. In the current frame, let $\mathcal{H}$ be the set of channels whose $\hat{T}_{\text{off}} > T_{\text{frame}} + \mu$, where μ ($< T_{\text{frame}}$) is a small quantity that accounts for discrepancy in the estimated values of T_{off}. Within $\mathcal{H}$, the idle channel with the highest probability of remaining idle during the next frame is selected as a CCC. The selected CCC is broadcasted by the MD during the BP at the end of the current frame.

Adaptive Reporting Strategy–Motivated by the high switching speeds of the A/D converters deployed in software defined radio front-ends [25], we propose an adaptive reporting strategy wherein the time allocated to the reporting phase (T_{rep}) is decided dynamically based on the number of channels scheduled for sensing/probing. Assume that r channels were scheduled by the MD. We equally divide T_{rep} into r sub-slots, one for each channel. In addition, the MD broadcasts a hopping sequence to rendezvous with the devices to gather the report packets. This hopping sequence information is encapsulated in the sensing/probing scheduling packet. Assume that the hopping sequence is $C_1, C_2, \ldots, C_r$. The MD tunes to channel C_i during the ith sub-slot. Suppose that channel i is scheduled for sensing/probing by link j. If channel i is sensed to be idle, it will be probed. The destination device of link j will then send a control packet to the MD, containing the PU state of the channel along with its quality (in case of successful probe packet exchange) during the ith sub-slot. Note that if a channel was sensed to be busy by link j, no control packet is sent during the ith sub-slot. Consequently, the MD interprets this channel to be occupied, and excludes it when assigning channels for data communication. The major accomplishment in this reporting strategy is the elimination of channel contention delay, which might hinder the timely exchange of vital control information. The MD waits for $t_{\text{rep}} \stackrel{\text{def}}{=} T_{\text{rep}}/r$ at each sub-slot for hearing any control packets from the associated SUs. If this time expires, the MD gracefully moves to the next sub-slot in T_{rep}.

VII. Performance Evaluation

A. Evaluation Setup

We consider an area of 50×50 m^2, mimicking an indoor environment. We consider 40 channels in the UHF band, each of 6 MHz bandwidth. Each channel can support one of five rates viz. 2, 4, 8, 12, and 16 Mbps, each with probability 0.2. This randomness in the channel data rate captures wireless phenomena like fading, shadowing, and RF interference in our simulations. We use the approximation used in [26] to capture τ_c in our simulations. Specifically, $\tau_c(t) = \frac{9\lambda}{16\pi v(t)}$, where $v(t)$ represents the velocity of the CR transmitter towards the intended CR receiver along the line of sight, and $\lambda = \frac{c}{f_c}$ represents the wavelength of the signal corresponding to the carrier frequency f_c. We vary τ_c uniformly between 1 and 10 secs. $T_{\text{on}} = T_{\text{off}} = 5$ secs.

TABLE I: Durations of various operations in the TDMA frame.

Operation	Duration (MAS)	Operation	Duration (MAS)
Association	5	Channel Reporting	25
Beacon Period	2	Channel Assignment	2
S/P Scheduling	2	Second-round Probing	3

As elucidated earlier, we resort to a frame-based time-slotted protocol. The time slots can be described at the medium-access level using MASs, with the duration of each MAS defined to be 1 msec in our setup. The fixed number of MASs allocated for each operation in our TDMA frame is illustrated in Table I. $T_{\text{frame}} = 250$ MASs. Each link carrying HP flow is randomly assigned a rate demand between 5 and 15 Mbps. The rate demands of the HP flows are updated once they complete transferring their video flows of predefined durations, as dictated by the video trace-files. P_d and P_{fa} are set to 0.9 and 0.25, respectively. β in Section IV is set to 0.75. All LP flows are composed of constant bit rate (CBR) traffic with constant data-packet size of 1 K byte. We use a 500 byte control packet. All simulations are carried out for 10000 frames using CSIM (a C-based process-oriented discrete-event simulation package), and reported values are the average of 20 runs. The optimization problems are solved using MATLAB. Our simulations are conducted to evaluate the performance gain resulted from the interactions between the various proposed components: QASPA, AFS, and the adaptive channel assignment strategy. All the three components contribute to the enhancement in the network performance achieved by the proposed protocol.

B. Evaluation of QASPA

1) Impact of QASPA on Discovery Efficiency: We study the discovery efficiency, defined as the number of idle channels discovered per unit time, achieved by QASPA and contrast it with a random scheduling scheme which does not make use of the estimated PU profiles and prior channel quality information while scheduling links for sensing/probing. This random scheduling is very similar to the channel probing scheme in [2]. Note that we allow unique sets of channels to be sensed/probed by individual links even under the random scheduling scheme, so as to prevent probe packet collision during the spectrum discovery phase. $T_{s,\max} = 20$ msecs and $\kappa = 2$ Mbps. $R_d = 3$ Mbps for all HP flows. Fig. 8 shows that the number of operational links has a profound impact on the discovery efficiency. Operation of sensing/probing processes in parallel boosts the discovery efficiency significantly. In contrast, random scheduling, despite being facilitated with parallel sensing/probing, fail to match the efficiency of QASPA due to the lack of knowledge on PUs profiles.

It is to be noted that the increase in discovery efficiency is also heavily attributed to the optimal ADTS scheme. To verify

this, we compare the discovery efficiency of STS, DTS, and the proposed ADTS and optimal ADTS schemes, for a single-link scenario under various values of $T_{s,\max}$. DTS scheme uses a fixed per-channel sensing duration. The uncertain region in DTS prevents us from accurately deciphering the PU state of the channel, and as a conservative approach we deem these channels to be busy. This results in lower discovery efficiency, as several channels, which might be idle, are deemed occupied. We break this norm in our ADTS scheme, wherein we use an adaptive per-channel sensing duration which helps us to accurately identify the PU state of the channel, thereby leading to improved sensing efficiency (defined as the ratio between the number of idle channels and the total number of channels sensed during $T_{s,\max}$), as seen in Fig. 9. Our optimal ADTS scheme further improves the sensing efficiency by optimizing the sensing time. In contrast to STS, ADTS, and optimal ADTS, the sensing efficiency of DTS changes abruptly with the discovery time. This happens because of the uncertainty region. With slight changes in the discovery time, several channels that had 'certain' states might fall in the uncertainty region, and vice versa. Although the uncertainty region also exists in the ADTS and 'optimal ADTS' schemes, the adaptability of the maximum per-channel sensing time in these schemes makes them immune to such abrupt changes.

In Fig. 10, we provide a more detailed comparison between the various sensing schemes. The total number of channels in the system is 60. Fig. 10(a) shows the total number of sensed channels as a function of the discovery time when $P_{md} = 0.1$ and $P_{fa} = 0.25$. Fig. 10(b) shows the number of sensed channels that are found idle and Fig. 10(c) shows the number of sensed channels that are found busy (both as a function of the discovery time). It is important to note that in contrast to all other sensing schemes, the sum of the idle and busy channels in the DTS scheme does not equal to the total number of sensed channels. In DTS, some of the sensed channels are neither idle nor busy (i.e., the total received energy over these channels falls in the uncertainty region). As shown in Fig. 10, the total number of sensed channels that result in a certain outcome (i.e., the number of idle channels, shown in Fig. 10(a), plus the number of busy channels, shown in Fig. 10(b)) is significantly higher in ADTS compared to STS and DTS. Optimal ADTS further improves this total number of sensed channels with a certain outcome compared to ADTS. Note from Fig. 10(a) that in DTS all channels can be sensed within $10\mu s$ while satisfying the required P_{md} and P_{fa} (this is inline with Fig. 5). In the other sensing schemes (STS, ADTS, and optimal ADTS), the number of sensed channels increases with the discovery time. As shown in Fig. 10(a), the number of sensed channels in STS is very small because it requires a significantly larger sensing time to satisfy the required P_{md} and P_{fa} compared to the DTS-based schemes (i.e., DTS, ADTS, and optimal ADTS).

Next, we compute the bandwidth discovered by QASPA to illustrate the impact of considering the channel quality in the sensing/probing scheduling. In this experiment, we fix the number of HP flows to 10, and vary R_d of each HP flow from 5 to 15 Mbps. Fig. 11 shows that the bandwidth discovered by random scheduling is much less than that of QASPA. Fig. 12 shows the significant reduction in the flow blocking

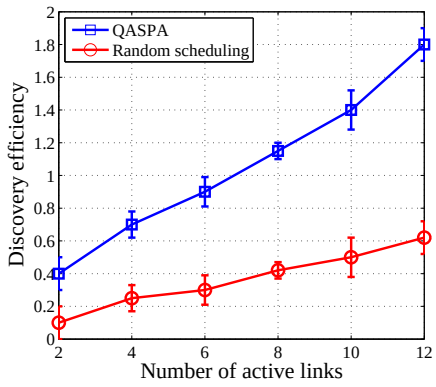

Fig. 8: Discovery efficiency of QASPA ($T_{s,\max} = 20$ msecs and $\kappa = 2$ Mbps. $R_d = 3$ Mbps for all HP flows).

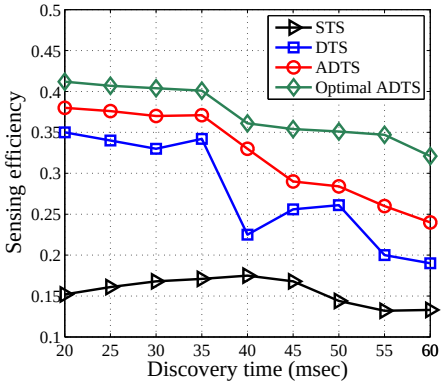

Fig. 9: Sensing efficiency ($T_{s,\max} = 20$ msecs and $\kappa = 2$ Mbps. $R_d = 3$ Mbps for all HP flows).

rate achieved by QASPA as a function of R_d.

Unlike other related works, we propose a complete end-to-end architecture to support bandwidth-intensive applications in CRNs. To the best of our knowledge, this is the first work to propose one such comprehensive solution to support high-bandwidth communications in CRNs. Thus, in order to accurately project the efficiency of our overall architecture, we had to compare the proposed components of our architecture with base models.

2) Impact of κ on QASPA: κ plays a very important role in mobile wireless networks, wherein the quality of the channel changes frequently due to node mobility. To evaluate the impact of κ on network throughput, we consider 10 HP and 5 LP flows. $T_{s,\max}$ is set to 20 milliseconds. Fig. 13 illustrates the impact of κ on the network throughput for two different rate demands. It is clear that the network throughput exhibits an upward trend for increasing κ in both scenarios until it reaches a breaking point, beyond which it starts decreasing.

Increasing κ beyond a certain limit prevents the scheduler from scheduling channels for the links to discover the high bandwidth requirement of $R_d + \kappa$ in a restricted spectrum

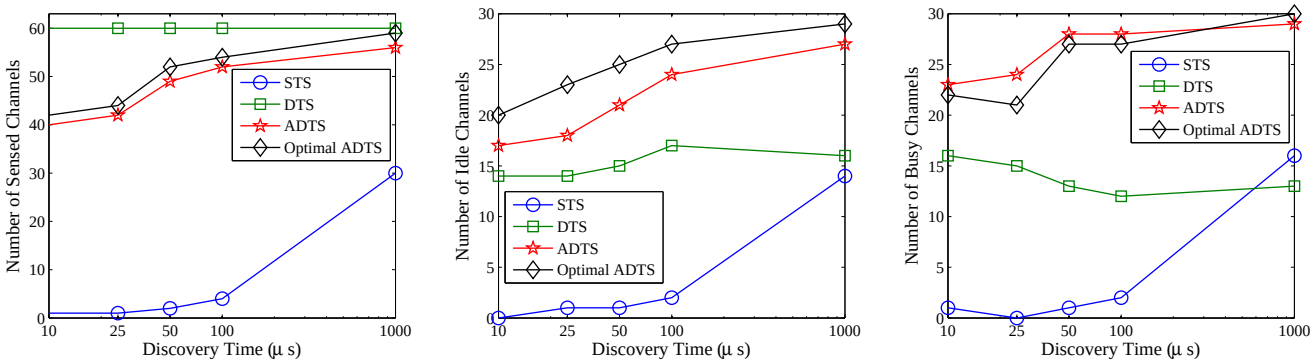

Fig. 10: Number of (a) sensed, (b) idle, and (c) busy channels vs. the discovery time ($P_{md} = 0.1$ and $P_{fa} = 0.25$).

discovery duration, leading to the links being dropped from data communication. In turn, these links sense unique channels during the spectrum discovery phase to improve the accuracy of the estimated PU usage profiles. Subsequently, these dropped links get associated during the occurrence of next S/P-1 frame. This experiment illustrates the need to choose an optimal value of κ during the operation of the protocol. Based on our experiment, we recommend κ to be ~ 2.5 Mbps to overcome the impact of channel quality fluctuation in a relatively low mobile environment. Fig. 14 clarifies that the observed throughput plunge in the previous experiment was because of links getting dropped owing to their high demands. It is interesting to note that positive values of κ might not be suitable in all cases, as the channel quality can improve from the previously measured instant, in which case we need to choose negative values for κ. However, our protocol is designed in a way that the excess opportunities can be used to serve unsatisfied HP flows via second round probing process.

C. Evaluation of AFS

1) Reduction in Control Overhead: Control overhead is the ratio of control packets to the total network packets exchanged over the entire simulation time. In our protocol, fast PU dynamics and low τ_c induce higher control packet generation. To evaluate the reduction in control overhead achieved by AFS, we conduct two experiments. First, we steadily increase the channel vacancy factor $\zeta \stackrel{\text{def}}{=} \hat{T}_{\text{off}}/(\hat{T}_{\text{on}} + \hat{T}_{\text{off}})$ over all channels in the system while fixing τ_c at 5 seconds. The rate demands of all HP flows is set to 7 Mbps with κ set to 2 Mbps. Fig. 15 shows the reduction in control overhead achieved by AFS over the ECMA-392, which uses fixed framing structure. Note that, the fixed framing structure used in our comparison is comparable with the OP-MAC protocol proposed in [3]. Increasing the number of HP flows increases the exchange of control packets in the network, as seen in Fig. 15. The adaptive nature of AFS helps in reducing the control overhead by $\sim 126\%$ when compared to the ECMA-392 frame design.

Second, we study the impact of τ_c on the control overhead by simulating 10 HP flows, each with $R_d = 7$ Mbps and $\kappa = 2$ Mbps. ζ is set as 0.5. A small value of τ_c implies high mobility and hence high channel quality variations, which invariably induces higher control packet exchanges. Fig. 16 illustrates the drastic reduction in the control overhead achieved by AFS.

2) Impact on Network Throughput: The reduction in the control overhead achieved by AFS allows us to increase the network throughput by up to 460% due to the increased use of D frames. For large number of HP flows, Fig. 17 clearly shows that AFS helps in improving the network throughput significantly, thereby making our protocol tailor made for supporting multiple HP flows simultaneously. As a result, Figs. 18 and 19 show the significant reduction in the flow blocking rate and admission delay achieved by our protocol. The high blocking rate and admission delay of ECMA-392 are due to the random nature of scheduling and channel allocation, which result in many links left unsatisfied. It is to be emphasized that the entire proposed architecture is simulated to obtain the results in Figs. 15- 19.

D. Evaluation of Adaptive Channel Assignment Strategy

1) Impact of Channel Bonding/Aggregation Techniques: Efficiency of channel bonding/aggregation in supporting HP flows can be readily seen in Fig. 20 wherein we simulate 10 HP and 5 LP flows. We set ζ to 0.5. In this experiment, we compare three schemes viz. best single-channel transmission, assignment based on channel bonding/aggregation without using second round of probing, and assignment based on channel bonding/aggregation augmented with second round of probing. The best single-channel transmission scheme tries to accommodate the HP flow over the channel which exhibits highest data rate among the ones discovered through channel probing. This scheme tries to emulate the "high preference" channel maintained at each node in MMAC protocol [27]. However, in our case, the "best single-channel" is chosen based on the supported data rate rather than channel occupancy. The best single-channel transmission scheme closely follows the proposed channel assignment strategy when the rate demands of the HP flows are relatively low. We can see a sharp dip in throughput with increase in R_d as the increased bandwidth

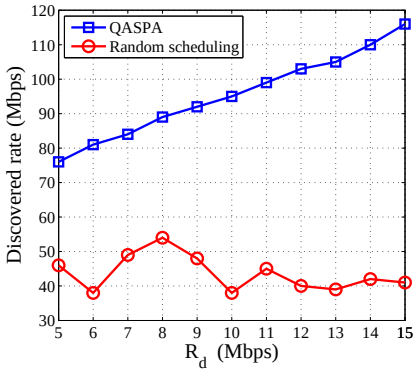

Fig. 11: Bandwidth discovered by QASPA ($L = 10$).

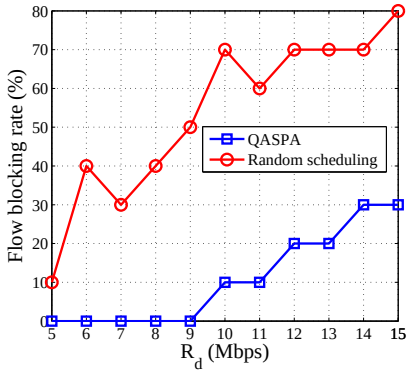

Fig. 12: Flow blocking rate vs. R_d ($L = 10$).

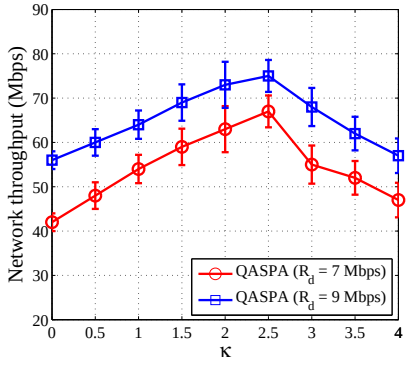

Fig. 13: Network throughput vs. κ (10 HP and 5 LP flows. $T_{s,\max} = 20$ msecs).

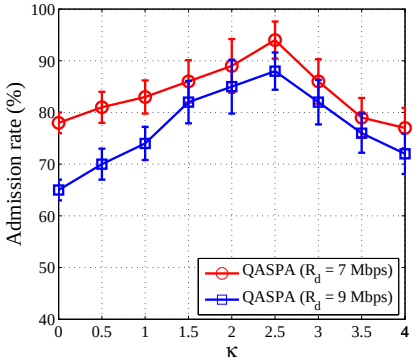

Fig. 14: Admission rate vs. κ (10 HP and 5 LP flows. $T_{s,\max} = 20$ msecs).

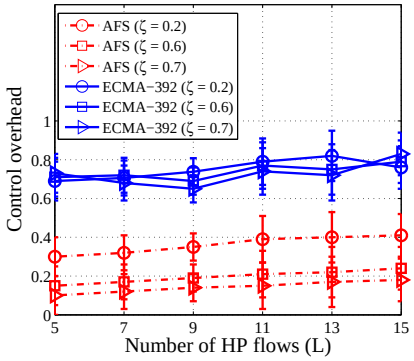

Fig. 15: Control overhead vs. L ($\tau_c = 5$ secs, $R_d = 7$ Mbps, and $\kappa = 2$ Mbps).

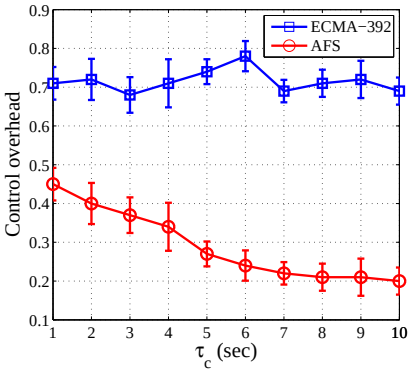

Fig. 16: Control overhead vs. τ_c (10 HP, $R_d = 7$ Mbps, $\kappa = 2$ Mbps, & $\zeta = 0.5$).

requirement can no longer be accommodated in a single narrow-band channel leading to the flow being dropped. This observation is very unappealing given the requirements imposed by current high-bandwidth applications. Channel bonding/aggregation scheme helps in significantly improving the throughput as the value of R_d increases by bundling together the available resources. One interesting observation made in Fig. 20 is the minor reduction in throughput by using second round channel probing when the value of R_d is relatively low. This demonstrates the slight increase in overhead introduced by second round channel probing process leading to a minor reduction in throughput. However, Fig. 20 also demonstrates the increase in throughput brought in by deploying second round probing process when the value of R_d is high. However, as the value of R_d increases, the efficiency of second round channel probing becomes prominent as we clearly observe improvement in network throughput as shown in Fig 20.

2) Impact of Second Round Channel Probing: Second round channel probing often acts as a decider when it comes to supporting multiple HP flows with very high demands. When the PU activity is high over all channels, the number of idle channels at any given instant is reduced, as a result several links might not be able to meet their demands by solely relying on the opportunities discovered by them. In such a scenario second round channel probing proves to be beneficial as seen in Fig. 21. Thus, channel assignment based on aggregation/bonding augmented with second round channel probing can be very useful when multiple HP flows need to be supported over a CRN exhibiting high PU activity.

E. Evaluation of Constrained Sensing/Probing Scheduling and Channel Assignment Strategies

In this section, we evaluate the throughput and admission rate of the constrained scheduling and assignment strategies proposed in Sections V-C and VI-B. Recall that $\mathcal{C}$ is the maximum number of channels that can be bonded/aggregated and $\mathcal{B}$ is the maximum allowable separation between the aggregated channels.

Similar to Figs. 13 and 14, Figs. 22 and 25 show that both the throughput and admission rate exhibit an upward trend with κ until it reaches a breaking point, beyond which they start decreasing. Relaxing the scheduling and assignment constraints by increasing $\mathcal{C}$, $\mathcal{B}$, or both improves the throughput and admission rate. Fig. 23 shows the significant throughput

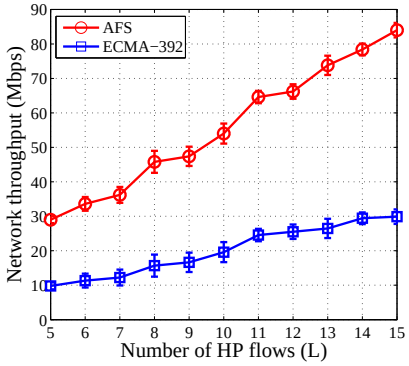

Fig. 17: Network throughput vs. L ($\tau_c = 5$ secs, $R_d = 7$ Mbps, and $\kappa = 2$ Mbps).

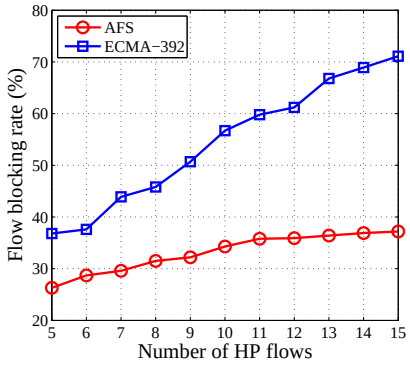

Fig. 18: Flow blocking rate vs. L ($\tau_c = 5$ secs, $R_d = 9$ Mbps, and $\kappa = 2$ Mbps).

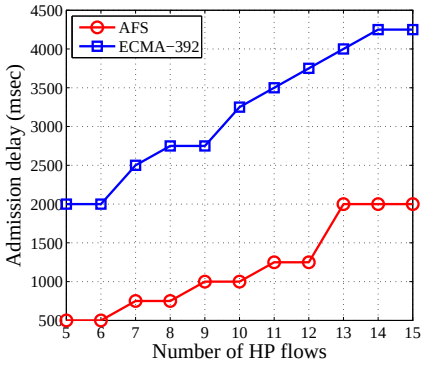

Fig. 19: Admission delay vs. L ($\tau_c = 5$ secs, $R_d = 9$ Mbps, and $\kappa = 2$ Mbps).

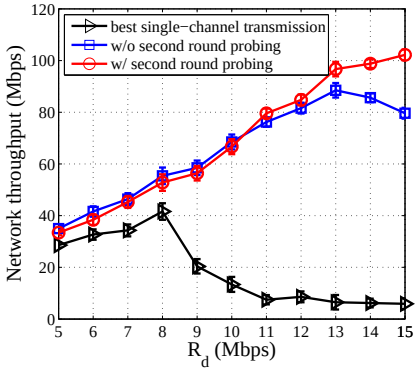

Fig. 20: Network throughput vs. R_d (10 HP and 5 LP flows and $\zeta = 0.5$).

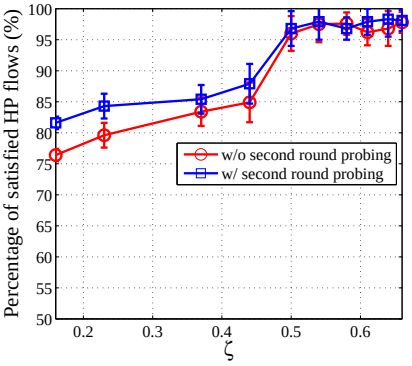

Fig. 21: Impact of second round probing (10 HP and 5 LP flows. $R_d = 5$ Mbps).

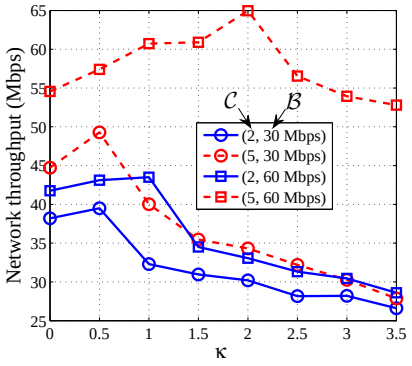

Fig. 22: Network throughput vs. κ (10 HP and 5 LP flows. $R_d = 9$ Mbps and $T_{s,\max} = 20$ msecs).

gain achieved by our protocol as compared with ECMA-392, even when the constrained scheduling and assignment schemes are used. As shown in Fig. 24, channel bonding/aggregation helps in significantly improving the throughput as the value of R_d increases when $\mathcal{C}$ is large enough ($\mathcal{C} = 5$ in the figure). When $\mathcal{C}$ is very small ($\mathcal{C} = 2$ in the figure), the throughput increases slowly with R_d up to a certain value, beyond which it remains the same. As a result, when $\mathcal{C}$ is very small, the admission rate decreases rapidly with R_d, as shown in Fig. 27. Fig. 26 shows the significant reduction in the admission rate as L increases when the constrained scheduling and assignment schemes are used, as compared to Fig. 18 in which channel bonding/aggregation is unconstrained.

VIII. Conclusions

Supporting bandwidth-intensive traffic over CRNs has always allured the research community. We proposed a framework to guarantee the rate demands of multiple high-bandwidth flows in a centralized setup by designing several efficient spectrum exploration and exploitation strategies. We advocated a technique to drastically reduce the control overhead in frame-based systems, so as to improve the network throughput. We also proposed an efficient channel allocation strategy, employing channel bonding and aggregation, which proved to be fruitful in increasing the throughput. Finally, we designed an optimal adaptive double-threshold based sensing policy, which was shown to drastically improve the spectrum sensing efficiency.

References

[1] P. Rysavy, "Spectrum crisis?" *Information Week Magazine*, pp. 23–30, 2009.

[2] A. Giannoulis, P. Patras, and E. W. Knightly, "Mobile access of wide-spectrum networks: Design, deployment and experimental evaluation," in *Proc. of the IEEE INFOCOM Conf.*, April 2013, pp. 1708–1716.

[3] D. Xue, E. Ekici, and X. Wang, "Opportunistic periodic MAC protocol for cognitive radio networks," in *Proc. of the IEEE GLOBECOM Conf.*, Dec. 2010, pp. 1–6.

[4] "MAC and PHY for operation in TV white space," *ECMA-392, second edition*, June 2012.

[5] Q. Zhao, S. Geirhofer, L. Tong, and B. Sadler, "Opportunistic spectrum access via periodic channel sensing," *IEEE Transactions on Signal Processing*, vol. 56, no. 2, pp. 785–796, 2008.

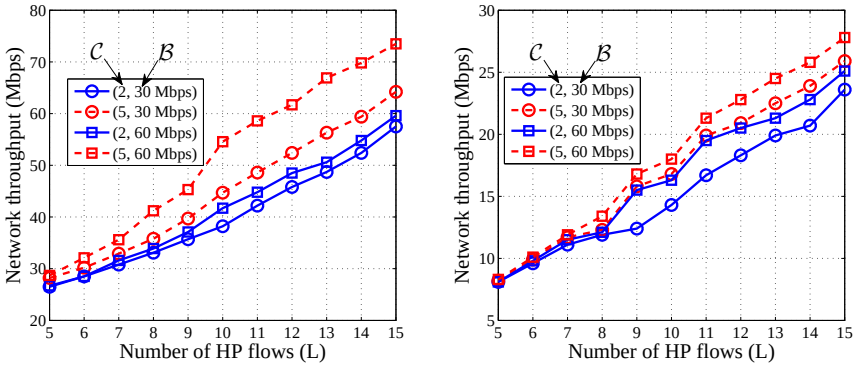

(a) AFS (b) ECMA-392

Fig. 23: Network throughput vs. L ($\tau_c = 5$ secs, $R_d = 9$ Mbps, and $\kappa = 2$ Mbps).

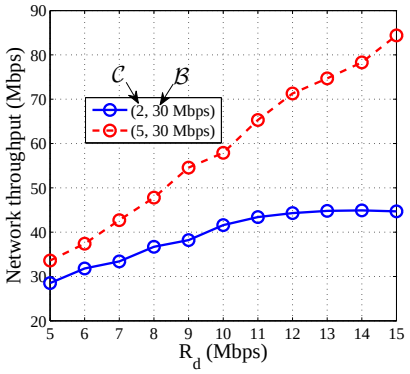

Fig. 24: Network throughput vs. R_d (10 HP and 5 LP flows and $\zeta = 0.5$).

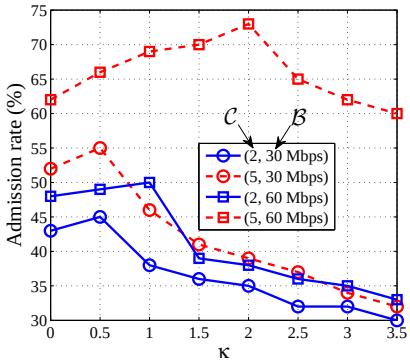

Fig. 25: Admission rate vs. κ (10 HP and 5 LP flows. $R_d = 9$ Mbps and $T_{s,\max} = 20$ msecs).

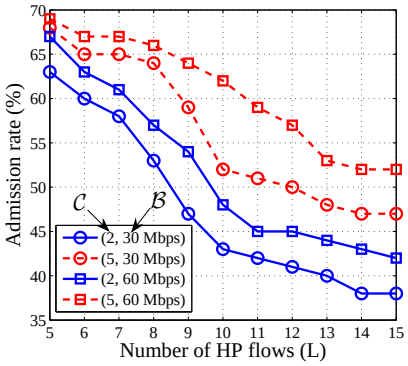

Fig. 26: Admission rate vs. L ($\tau_c = 5$ secs, $R_d = 7$ Mbps, and $\kappa = 2$ Mbps).

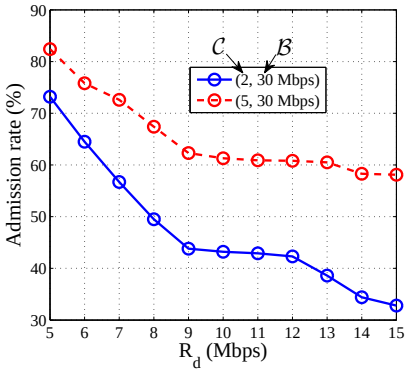

Fig. 27: Admission rate vs. R_d ($L = 10$).

[6] R. Choudhury, X. Yang, R. Ramanathan, and N. Vaidya, "On designing MAC protocols for wireless networks using directional antennas," *IEEE Transactions on Mobile Computing*, vol. 5, no. 5, pp. 477–491, May 2006.

[7] H. Bany Salameh, M. Krunz, and O. Younis, "Cooperative adaptive spectrum sharing in cognitive radio networks," *IEEE/ACM Transactions on Networking*, vol. 18, no. 4, pp. 1181–1194, Aug. 2010.

[8] T.-S. Kim, H. Lim, and J. C. Hou, "Improving spatial reuse through tuning transmit power, carrier sense threshold, and data rate in multihop wireless networks," in *Proc. of the ACM MobiCom Conf.*, 2006, pp. 366–377.

[9] J. Zhu, Z. Xu, F. Wang, B. Huang, and B. Zhang, "Double threshold energy detection of cooperative spectrum sensing in cognitive radio," in *Int'l Conf. on Cognitive Radio Oriented Wireless Networks and Communications*, 2008, pp. 1–5.

[10] J. Jafarian and K. Hamdi, "Throughput optimization in a cooperative double-threshold sensing scheme," in *Proc. of the IEEE WCNC Conf.*, 2012, pp. 1034–1038.

[11] T. S. Ferguson, *Optimal stopping and applications*. [Online]. Available: http://www.math.ucla.edu/ tom/Stopping/Contents.html.

[12] N. Chang and M. Liu, "Optimal channel probing and transmission scheduling for opportunistic spectrum access," *IEEE/ACM Transactions on Networking*, vol. 17, no. 6, pp. 1805–1818, 2009.

[13] T. Bansal, B. Chen, and P. Sinha, "DISCERN: Cooperative whitespace scanning in practical environments," in *Proc. of the IEEE INFOCOM Conf.*, April 2013, pp. 719–727.

[14] H. Kim and K. Shin, "Fast discovery of spectrum opportunities in cognitive radio networks," in *Proc. of the IEEE DySPAN Conf.*, Oct. 2008, pp. 1–12.

[15] A. Kumar, K. G. Shin, Y. J. Choi, and D. Niculescu, "On time-domain coexistence of unlicensed and licensed spectrum users," in *Proc. of the IEEE DySPAN Conf.*, Oct 2012, pp. 223–234.

[16] P. Bahl, R. Chandra, T. Moscibroda, R. Murty, and M. Welsh, "White space networking with Wi-Fi like connectivity," in *Proc. of the ACM SIGCOMM Conf.*, Aug. 2009, pp. 27–38.

[17] Y.-C. Liang, Y. Zeng, E. C. Y. Peh, and A. T. Hoang, "Sensing-throughput tradeoff for cognitive radio networks," *IEEE Transactions on Wireless Communications*, vol. 7, no. 4, pp. 1326–1337, April 2008.

[18] F. Digham, M.-S. Alouini, and M. Simon, "On the energy detection of unknown signals over fading channels," in *Proc. of the IEEE ICC Conf.*, May 2003, pp. 3575–3579.

[19] S. O. Krumke, *Integer Programming: Polyhedra and Algorithms*. [Online]. Available: http://staff.guilan.ac.ir/staff/users/salahi/fckeditor_repo/file/ip-lecture-new.pdf.

[20] K. Bian, J.-M. Park, and R. Chen, "Control channel establishment in cognitive radio networks using channel hopping," *IEEE Journal on Selected Areas in Communications*, vol. 29, no. 4, pp. 689–703, 2011.

[21] M. J. Abdel-Rahman, H. Rahbari, and M. Krunz, "Adaptive frequency hopping algorithms for multicast rendezvous in DSA networks," in *Proc. of the IEEE DySPAN Conf.*, Oct. 2012, pp. 517– 528.

[22] M. J. Abdel-Rahman, H. Rahbari, M. Krunz, and P. Nain, "Fast and secure rendezvous protocols for mitigating control channel DoS attacks," in *Proc. of the IEEE INFOCOM Mini-Conf.*, April 2013, pp. 370–374.

[23] M. J. Abdel-Rahman and M. Krunz, "Game-theoretic quorum-based frequency hopping for anti-jamming rendezvous in DSA networks," in *Proc. of the IEEE DySPAN Conf.*, April 2014, pp. 248–258.

[24] M. J. Abdel-Rahman, H. Rahbari, and M. Krunz, "Multicast rendezvous in fast-varying DSA networks," *IEEE Transactions on Mobile Computing*, 2014.

[25] A. Sampath, L. Yang, L. Cao, H. Zheng, and B. Y. Zhao, "High throughput spectrum-aware routing for cognitive radio networks," in *Proc. of the CROWNCOM Conf.*, 2007.

[26] V. Kanodia, A. Sabharwal, and E. Knightly, "MOAR: A multi-channel opportunistic auto-rate media access protocol for ad hoc networks," in *Proc. of the IEEE BroadNets Conf.*, Oct. 2004, pp. 600–610.

[27] J. So and N. H. Vaidya, "Multi-channel MAC for ad hoc networks: Handling multi-channel hidden terminals using a single transceiver," in *Proc. of the ACM MobiHoc Conf.*, 2004, pp. 222–233.